A Review on 3-D Magnetic Property Testing System for Measuring Rotational Core Loss of Soft Magnetic Materials

Ashraf Rohanim Asari, Youguang Guo, *Senior Member, IEEE*, Jianguo Zhu, *SeniorMember, IEEE*
Faculty of Engineering and Information Technology
University of Technology, Sydney (UTS)
Broadway NSW 2007, Australia

Fatimah Sham Ismail
Centre for Artificial Intelligence & Robotics (CAIRO)
Universiti Teknologi Malaysia, Jalan Semarak,
54100 Kuala Lumpur, Malaysia

Abstract—**In today's world, the development of electromagnetic devices require the magnetic cores to be operated at higher frequency. Soft magnetic composite (SMC) materials are suitable for these applications because of their properties like high electrical resistivity which leads to the low eddy current loss, and 3-D magnetic isotropy which provides great design flexibility of various electromagnetic devices. On top of that, the prediction of core losses is very important in obtaining the optimum design of the electrical machines which is always aiming for high efficiency. This paper reviews the development of 3-D magnetic property testing system or 3-D tester in studying the rotational core loss of SMC materials based on the previous researches in the last decade.**

Keywords—electromagnetic devices; soft magnetic composite (SMC) materials; core loss; efficiency; 3-D magnetic property testing system

I. INTRODUCTION

For over a century, soft magnetic materials have been adopted in various scientific and commercial applications by on-going technology development. These materials are suitable in fabricating core components of electromagnetic devices due to their properties. Among various soft magnetic materials, SOMALOY^{TM} 500 is a soft magnetic composite (SMC) material that has been developed by Hoganas AB, Sweden which uses a highly pure iron particle with surface coating to ensure low eddy current loss and 3-D magnetic isotropy. It is really demanded by the motor development nowadays in obtaining high performance and low cost electromagnetic devices with 3-D magnetic flux, such as claw pole and transverse flux machines [1-5].

To develop high performance electromagnetic devices, accurate modelling of the magnetic properties, such as core loss, is crucial. Some models of core losses have been developed for predicting the core loss of the SMC materials based on measurement on material samples under 1-D alternating and 2-D rotating magnetic excitations [6-10], and have been applied in designing various electrical machines with SMC cores [11][12]. This paper aims to review the magnetic measurement under 3-D vector magnetic excitations by using 3-D magnetic property measurement system. Both alternating and rotational core losses can be measured by using the 3-D tester. Measuring apparatus has been studied and improved in order to obtain the accurate reading by using the appropriate techniques and procedures.

II. MEASUREMENT APPARATUS OF CORE LOSS MEASUREMENT

A. *3-D magnetic property testing system*

Each magnetic material that is excited under an alternating or rotating magnetic field has been experienced on the rotation of magnetic domain, so the 3-D vector flux excitation should also be considered [13]. In 2001, Zhong and Zhu proposed the 3-D magnetic property testing system in order to study the magnetic properties under 3-D excitation of vector fluxes [14]. The 3-D magnetic property testing system was successfully developed by Zhu *et al.* in 2003 for magnetizing cubic samples of soft magnetic materials [14]. This system consists of a 3-D yoke, a data acquisition system, the sample in the centre of the system and three groups of coils to produce magnetic field *B* along the orthogonal *x-, y-* and *z-* axes, respectively. The tester is able to produce different magnetic flux patterns such as alternating, rotating in a plane and rotating in a 3-D pattern [13-18]. The 3-D tester has also been attached with a feedback control system which contains a control unit and three high power amplifiers [15].

As shown in Fig. 1, the voltage waveforms of magnetic flux density for the *x-, y-* and *z*-components are generated by the function generator, and exported to a three channel linear power amplifier, which feeds the excitation windings of the tester, through three isolated channels of the A/D and D/A board [13][14]. The *x-, y-* and *z*-components of B and H sensing coils generate voltage signals, which are collected by six independent input channels of the A/D and D/A board. The signals are used to determine the relationship of *B* and *H* in order to calculate the core loss of the sample. The signals of *B* are also used for feedback control of the waveforms. By using this tester, some measurement results with cubic SMC samples have been obtained and analysed under 1-D alternating excitation along one axis, 2-D circularly or elliptically rotating on a plane, e.g. XOY, YOZ or ZOX, which can be considered as quasi-3-D measurements, and real 3-D measurements, e.g. the tip of B is controlled to form a sphere [19].

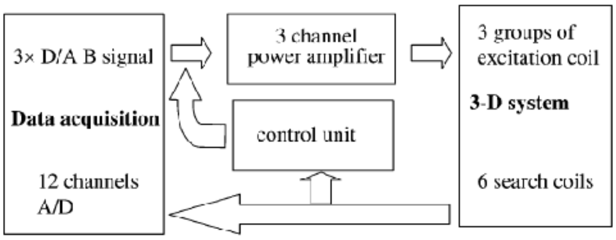

Fig. 1. 3-D magnetic property testing system [19].

B. Calibration of Sensing Coil

The sample surface field intensity components H_x, H_y, and H_z are measured by twelve H search coils while the flux density through the sample cross sections B_x, B_y and B_z are measured by three B search coils that have been wrapped around the cubic sample [14]. Each surface of cubic sample has two H search coils (H_x and H_y) and one B search coil (B_z) which lead to twelve coils for H and six coils for B [14], [20] as illustrated in Fig. 2.

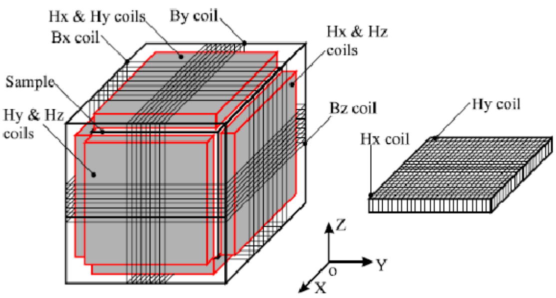

Fig. 2. A cubic sample and its B and H sensing coils [14].

Induced electromotive force (EMF) of the search coils can be used in computing the components of magnetic field intensity H and magnetic flux density B on each axis. For (2) and (4), the coil coefficients, K_H and K_B, would be determined to calculate the magnetic field at the sample surface. The coil coefficients can be obtained by conducting a calibration in a long solenoid. Calibration of sensing coil was studied considering the following equations. The calibration process is important in order to eliminate the system errors before being employed to measure the magnetic field components in the 3-D magnetic properties testing system [15].

$$B_i = \frac{1}{K_{B_i}} \int V_{B_i} dt \qquad (1)$$

$$K_{B_i} = N_{B_i} A_{sp} \qquad (2)$$

$$H_i = \frac{1}{\mu_0 K_{H_i}} \int V_{H_i} dt \quad (i=x,\ y,\ z) \qquad (3)$$

$$K_{Hi} = \frac{V_H}{\sqrt{2}\pi f \mu_0 H_m} \qquad (4)$$

where V is the RMS value of the induced EMF, $\mu_0 H_m$ is the peak value of the flux density in the centre of the solenoid, f is the excitation frequency, and A_{sp} is the cross-sectional area of the sample.

C. Improvement of the sensing coils

In 2009, Li *et al.* improved the original structure of 3-D tester by revising the size of the H coil to be in minimum area (8.5 x 6) mm^2 in order to acquire the accurate measurement. Two layers of coils with a small cross angle are able to induce signals with the same magnitude but in different direction [21].

The improved structure combines six H coils and six B coils as shown in Fig. 3. The very thin and small circle of 60 turns B coil is embedded in the centre of the epoxy resin frame while 200 turns H coil is wound around a 0.5 mm thick epoxy resin and covers the B coil [21-23]. The 0.05 mm enamelled copper wire is used for both B and H sensing coils to reduce the measurement error. Unwanted stray field will induce the additional EMF and adoption of cross bedded winding structure and twisted terminal are able to eliminate it [22][23]. Moreover, the twisted terminal of each coil would be able to reduce the error induction [22][23].

In Fig. 4, six combination sets of H coils and B coils are attached at each surface of cubic sample and this will drive for coils on the opposite sides and connected in series arrangement [21]. In order to obtain the uniform magnetic field at the sample, the H coils would be closely attached to the sample.

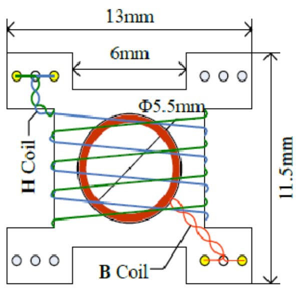

Fig. 3. Improved structure of H coils and B coils [21].

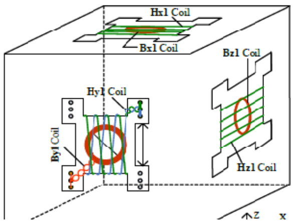

Fig. 4. Sample with sensing coils [21].

D. *Improvement of the exciting winding coils*

Adjustable multilayer excitation coils are discussed by Li *et al.* in 2010 to overcome the limitation of frequency operation [24]. The original excitation coils are redesigned to cover three ranges of frequency which cater for 2 Hz to 1000 Hz as illustrated in Fig. 5 [24]. In Fig. 5, each 16-layer winding includes three coils which consists of 2-layer coil for No. 1, 6-layer coil for No. 2, and 8-layer coil for No. 3, and each layer is designed to be 35 turns [24]. No.1 coil is for 200-1000 Hz, No. 1 and No. 2 coils are assigned for 20-200 Hz experiment, and all the three coils of No. 1, No. 2 and No. 3 are set to be in series for 2-20 Hz experiment as displayed in Fig. 6 [23].

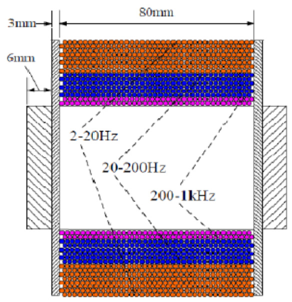

Fig. 5. Scheme of improved excitation coil [24].

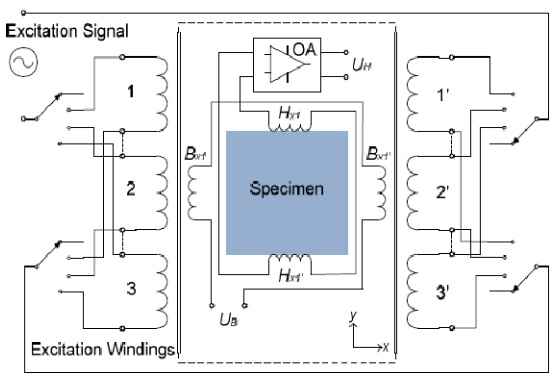

Fig. 6. Excitation and sensing structure in one axis [23].

Each pair of excitation windings are connected in series or parallel depending on the required frequency and impedance. Thus, both low and high frequency can be detected since each level of frequency has been assigned for the particular excitation coils and then will magnetize the specimen in different frequencies [23]. In high frequency, the impedance of the coil will be increased due to the increment of inductive reactance of the coil. A series RLC resonance circuit is adopted to compensate the phase angle between AC voltage and current. Besides that, the maximum excitation also can be obtained [23]. A series of RLC resonance is shown in Fig. 7 where L is the inductance of the selected excitation coil, R_L is the DC resistance of the excitation coil, C is the AC capacitor, R is the external resistance for impedance matching of the power amplifier outputs.

E. *Excitation circuit*

Fig. 6 illustrates the scheme of excitation and sensing structure in the x axis. It is also applied in the y and z axes. Experiment implementation for different typical frequency scope is performed by selecting the option switch of corresponding excitation coil [23]. The two exciting winding coils of x axis are connected in series with no phase angle difference to ensure the generation of maximum and uniform magnetic field inside the sample.

From the scheme of excitation and sensing structure, it can be seen that the operational amplifier (OA) is needed before data acquisition since the voltage of H signal is very small [23].

During the magnetization process, it is very important to consider the parameters of the excitation circuit since they will be designed in terms of frequency. When the frequency is higher, the impedance of the coil will be higher because of the inductive reactance X_L, and the voltage drop of the coil will be increased. A series RLC resonance circuit is adopted to compensate the phase angle between AC voltage and current and obtain maximum excitation current [23].

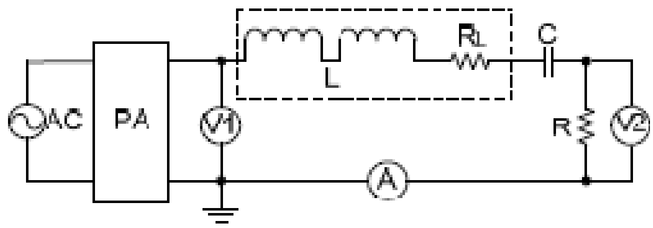

Fig. 7. Excitation circuit with RLC resonance [23].

Fig. 7 displays the part of excitation coil that implies a series of RLC circuit where L is inductance of the selected coil, R_L is the DC resistance of the excitation coil, C is the AC capacitance, and R is the external resistance for impedance matching of the power amplifier (PA) outputs. The wide range frequency experiment parameters are shown in Table 1 [23].

TABLE 1. PARAMETERS IN THE WIDE RANGE FREQUENCY [23].

PARAMETERS OF THE WIDE-RANGE-FREQUENCY EXPERIMENTS

f (Hz)	L (H)	N (Turns)	C (μF)	R_L (Ω)	R (Ω)
2	0.7742	1120	8180	3.6403	1
5	0.6178	980	1640	3.0537	1
20	0.2169	560	292	1.9384	2
50	0.1267	420	80	1.1927	1
100	0.1206	420	21	1.1927	1
200	0.0302	105	21	0.298	1
500	0.0291	105	3.48	0.2919	1
1000	0.0034	70	7.5	0.276	1.5

F. Development of guarding piece structure

Researchers have worked on the structure of 3-D tester in obtaining the high and uniform magnetic flux density production. In 2010, Li *et al.* applied the guarding piece structure to improve the uniformity of the magnetic field at the surface of the cubic specimen which leads to the high measurement accuracy [25]. The guarding pieces can significantly decrease the equivalent reluctance of the magnetic circuit and it is also able to reduce the required excitation current in magnetizing the test specimen [15][25]. This structure consists of six guard pieces that are made of the same material as the test specimen [25] as shown in Fig. 8. The sensing coils are located inside the structure and this will decrease the air gaps between core pole and specimen.

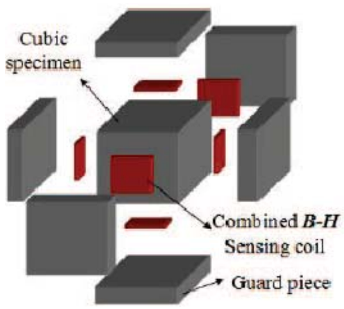

Fig. 8. Structure of guarding pieces: cubic sensing box with sample, sensing coils and guard piece [25].

Fig. 9 shows the distribution of magnetic flux density inside the test specimen with and without guarding pieces enclosed around the sensing coils. Magnetic flux density is higher and more uniform with adoption of homogeneous guarding pieces.

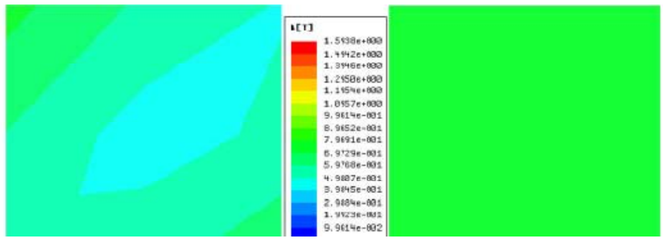

Fig. 9. Magnetic field distribution of the specimen without (left) and with (right) guarding pieces [26].

G. Development of "C-type" cores

After some improvements on the 3-D tester, Yang *et al.* (2014) realized that joints between cores and yoke of the original 3-D tester structure are not completely uniform which will influence the results of measurement due to the structural anisotropy. Considering that, the core-yoke structure has been improved by designing and modelling the "C-type" cores in the 3-D tester structure as shown in Fig. 10 in order to eliminate the influence of the connection disagreement between the laminated cores and yoke [22] and avoid an anisotropy structure [26]. There are three orthogonal "C-type" cores and six multilayer excitation windings, which are wound around the orthogonal core poles.

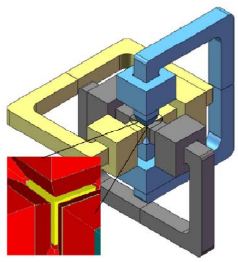

Fig. 10. Model of 3-D magnetization structure with "C-types" cores [26].

This novelty of cores is able to balance and smooth the path of the flux along the three axes.

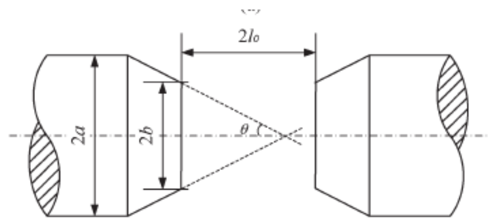

Fig. 11. Schematic frustum structure of the core pole [26].

From Fig. 11, it can be seen that the terminal of the core poles are shaped to be in frustum of a square pyramid in order to concentrate the magnetic flux density B [26]. The frustum core pole is proposed to generate a large air-gap magnetic flux density. More lines of magnetic force would be concentrated across the pole face, and the other fraction would pass through the conical surface which forms the concentrated magnetic field in the frustum of cone poles air gap [26]. The maximum magnetic flux density in the air gap can be formulated [26]

$$B_o = \mu_o M \left(1 - \frac{l_0}{\sqrt{{l_0}^2 + b^2}} \right) + M sin^2\theta \cos ln\frac{a}{b} \quad (5)$$

where *a* is the radius of the bottom circle, *b* is the radius of the upper circle, l_0 is the half length of the air gap, θ is the cone angle with the axis, and *M* is the magnetization intensity.

Fig. 12 shows the concentrated and uniform magnetic field in the centre of the structure after consideration into frustum of a square pyramid shape [26].

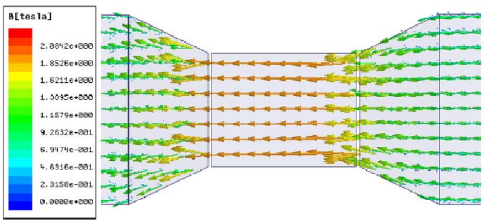

Fig. 12. Cross-section of B distribution in the magnetic concentration model [26].

III. CONCLUSION

The 3-D tester is the important system that is used to measure the 3-D magnetic properties of soft magnetic materials, which are then applied to estimate the core loss of the electromagnetic rotating devices under 3-D vector flux excitations at wide range of frequency. It is able to produce the 3-D vector flux excitation and magnetize the material sample which is located in the centre of the system. The development of multilayer excitation coils is formed to make the measurements to be operated at higher frequency up to 1000 Hz. Year by year, the researchers are trying to obtain the accurate core loss by determining the voltage signal of B and H through the magnetization process with the production of relatively uniform and high magnetic field. The guarding piece structure and C-types cores have been successfully developed in ensuring the sensing coils of B and H to be more sensitive in detecting the magnitude of magnetic field B and magnetic field strength H of the sample. Besides that, the calibration of sensing coils also has been improved in order to acquire the precise value of sensing box coefficients K_B and K_H. The improvements in core loss measurement are actively studied in the past decade to increase the energy efficiency of the system since the core loss is recorded as one of the main contributors of total loss in motor inefficiency. Fig. 13 summarizes the development of the 3-D magnetic property testing system. However, there is still a lack in measuring the core loss under the real 3-D vector flux excitation.

Considering the improved 3-D tester and the appropriate tool and method, the core loss of SMC material is planned to be measured under the real 3-D vector flux excitation by varying the magnitudes and phases of B along the x, y and z axes. This core loss measurement can be assumed as accurate due to the involvement of real 3-D excitation which is nature of the magnetic field in the electromagnetic devices.

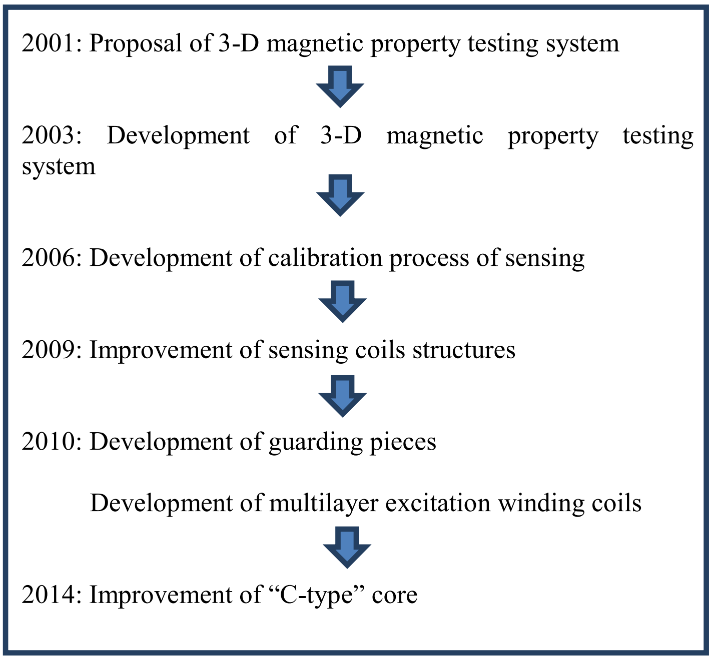

Fig. 13. Flow diagram of the development of 3-D magnetic property testing system structure.

REFERENCES

[1] Y. G. Guo and J. G. Zhu, “Magnetic field calculation of claw pole permanent magnet machines using magnetic network method,” *J. Elect. Electron.Eng., Australia*, vol. 22, no. 1, pp. 69–75, 2002.

[2] Y. G. Guo, J. G. Zhu, J. J. Zhong, and W. Wu, "Core losses in claw pole permanent magnet machines with soft magnetic composite stators", *IEEE Trans. Magn.*, vol. 39, no. 5, pp.3199 -3201 2003.

[3] Y. G. Guo , J. G. Zhu , Z. W. Lin and J. J. Zhong "Measurement and modeling of core losses of soft magnetic composites under 3D magnetic excitations in rotating motors", *IEEE Trans. Magn.*, vol. 41, no. 10, pp.3925 -3927 2005.

[4] P. Viarouge, J. Cros, and S. Clénet, “Design of inductors and transformers with soft magnetic composites,” in *Proc. Int. Conf. Electr.Mach.*, Brugge, Belgium, Aug. 2002, paper no. 514, CD-ROM.

[5] “The latest development in soft magnetic composite technology,” SMC Update, Reports of Höganäs AB Sweden, 1997–2007 [Online]. Available: http://www.hoganas.com.

[6] Y. G. Guo, J. G. Zhu, J. J. Zhong, H. Lu and J. Jin "Measurement and modeling of rotational core losses of soft magnetic materials used in electrical machines: A review", *IEEE Trans. Magn.*, vol. 44, no. 2, pp.279 -291 2008.

[7] J. G. Zhu, J. J. Zhong, V. S. Ramsden, and Y. G. Guo, “Power losses of composite soft magnetic materials under two dimensional excitations,” *J. Appl. Phys.*, vol. 85, no. 8, pp. 4403–4405, Apr. 1999.

[8] J. J. Zhong, “Measurement and modelling of magnetic properties of materials with rotating fluxes,” Ph.D. thesis, Univ. Technology, Sydney, Australia, Dec. 2002.

[9] J. J. Zhong, Y. G. Guo, J. G. Zhu, and Z. W. Lin, “Characteristics of soft magnetic composite material under rotating fluxes,” *J. Magn. Magn. Mater.*, vol. 299, no. 1, pp. 29–34, Apr. 2006.

[10] Y. G. Guo, J. G. Zhu, and J. J. Zhong, “Measurement and modelling of magnetic properties of soft magnetic composite materials under 2D vector magnetisations,” *J. Magn. Magn. Mater.*, vol. 302, no. 1, pp. 14–19, Jul. 2006.

[11] Y. G. Guo, J. G. Zhu and H. Lu "Design of SMC motors using hybrid optimization techniques and 3D FEA with increasing accuracy", *Proc. Int. Conf. Electr. Mach. Syst.*, vol. 3, pp.2296 -2301 2005.

[12] J. Cros , P. Viarouge and M. T. Kakhki "Design and optimization of soft magnetic composite machines with finite element methods", *IEEE Trans. Magn.*, vol. 47, no. 10, pp.4384 -4390 2011.

[13] J. J. Zhong and J. G. Zhu, “Electromagnetic design of a 3D tester for magnetic properties of soft magnetic materials,” Proc. 5th Int. Conf. Electr. Machines Syst., pp. 392 -395, 2001.

[14] J. G. Zhu, J. J. Zhong, Z. W. Lin, and J. D. Sievert, “Measurement of core losses with 3-D magnetic fluxes,” IEEE Transactions on Magnetics, vol. 39, pp. 3429-3431, 2003.

[15] Z. W. Lin, H. W. Lu, J. G. Zhu, J. J. Zhong, X. L. Wang, and S. Y. Ding, “Vector characterization of soft magnetic materials,” Journal of Applied Physics, vol. 97, 10R306-1-3. 2005.

[16] J. G. Zhu, J. J. Zhong, Z. W. Lin, and J. D. Sievert, “Measurement of magnetic properties under 3-D magnetic excitations,” IEEE Trans. On Magnetics, vol. 39, no. 5, pp. 3429-3431, 2003.

[17] Z. W. Lin, J. G. Zhu, and Y. G. Guo, “Three-dimensional hysteresis of soft magnetic composite,” J. Appl. Phys., vol. 99, paper 08D909, 2006.

[18] Y. G. Guo, J. G. Zhu, Z. W. Lin, and J. J. Zhong, “3D vector magnetic properties of soft magnetic composite material,” J. Magn. Magn. Mater., vol. 302, no. 2, pp. 511–516, Jul. 2006.

[19] Y. G. Guo, J. G. Zhu, Z. W. Lin, J. J. Zhong, H. Y. Lu, and S. H. Wang, “Calibration of sensing coils of a three-dimensional magnetic property tester,” IEEE Trans. Magn., vol. 42, pp. 3243 -3245, 2006.

[20] Y. G. Guo, J. G. Zhu, Z. W. Lin, J. J. Zhong, H. Y. Lu, and S. Wang, “Determination of 3-D magnetic reluctivity tensor of soft magnetic composite material,” J. Magn. Magn. Mater., vol. 312, pp. 458-463, 2007.

[21] Y. J. Li, Q. X. Yang, Y. H. Wang, J. F. Sun, J. G. Zhu, Y. G. Guo, Z. W. Lin, W. Xu, and Y. Wang, “Improved measurement of three-dimensional magnetic properties of SMC material,” in Applied Superconductivity and Electromagnetic Devices, International Conference, pp. 155-158, 2009.

[22] Y. J. Li, Q. X. Yang, J. G. Zhu, and Y. G. Guo, “Magnetic properties measurement of soft magnetic composite materials over wide range of excitation frequency,” IEEE Trans. Ind. Appl., vol. 48, no. 1, pp. 88-97, 2012.

[23] Y. J. Li, J. G. Zhu, Q. X. Yang, Z. W. Lin, W. Xu, and Y. Wang, “Magnetic properties measurement of soft magnetic composite materials over wide range of excitation frequency,” Energy Conversion Congress and Exposition (ECCE), 2010 IEEE, pp. 2259-2265.

[24] Y. J. Li, J. G. Zhu, Q. X. Yang, Z. W. Lin, Y. G. Guo, and Y. Wang, “Measurement of soft magnetic composite material using an improved 3D tester with flexible excitation coils and novel sensing coils,” IEEE Trans. Magn., vol. 46, no. 6, pp. 1971 -1974 2010.

[25] Y. J. Li, J. G. Zhu, Q. X. Yang, J. F. Sun, Y. Wang, and W. Xu, “Analysis of the 3-D magnetic reluctivity tensor based on magnetic properties measurement of SMC materials,” Electrical Machines and Systems (ICEMS), 2010 International Conference, pp. 1767-1772, Oct. 2010.

[26] Q. X. Yang, Y. J. Li, Z. H. Zhao, L. H Zhu, Y. Luo, and J. G. Zhu, “Design of a 3-D rotational magnetic properties measurement structure for soft magnetic materials,” Applied Superconductivity, IEEE Transactions, vol. 24, no. 3, pp. 1-4, June 2014.